

## RESEARCH ARTICLE

# Measurement and Analysis of Radar Signals Modulated by Flapping Wings of Birds

JIANGKUN GONG<sup>1</sup>, (Member, IEEE), DEREN LI<sup>1</sup>, (Senior Member, IEEE), JUN YAN<sup>1</sup>, HUIPING HU<sup>2</sup>, AND DEYONG KONG<sup>1,3</sup>

<sup>1</sup>State Key Laboratory of Information Engineering in Surveying, Mapping and Remote Sensing, Wuhan University, Wuhan 430079, China

<sup>2</sup>Wuhan Geomatics Institute, Wuhan 430022, China

<sup>3</sup>School of Information and Communication Engineering, Hubei University of Economics, Wuhan 430205, China

Corresponding author: Jun Yan (yanjun\_pla@263.net)

This work was supported by Wuhan University LIESMARS Special Research Funding under Grant 2020-2021.

This work involved human subjects or animals in its research. Approval of all ethical and experimental procedures and protocols was granted by the Laboratory Animal Use Protocol (AUP) from the IACUC of Wuhan University Center for Animal Experiment under IACUC Pre-Review No. WP20220122.

**ABSTRACT** There are arguments about the scattering mechanism of the 10-dB periodic signal fluctuations posed by the repetitive flapping motion in radar ornithology. We design a dynamic measurement system composed of a network analyzer and a high-speed camera to track dynamic radar signals modulated by the flapping gaits of birds within the S-band, X-band, and Ku-band. The results indicate that the respiration motion contributes little to the bird's signals, but the flapping wings not only contribute at least 10 dB to the signal fluctuation, but also modulate the radar signals of flying birds related to the flapping gaits, regarding different radar bands, observing angles and bird species. Furthermore, the contributions observed in the tests indicate that our theory of the time-varying wingbeat corner reflector (WCR) effect is correct in explaining the modulation mechanism of the 10-dB signal fluctuations in radar ornithology.


**INDEX TERMS** Bird radar signals, dynamic measurement, flapping wings, signal fluctuation, time-varying wingbeat corner reflector (WCR) effect.

## I. INTRODUCTION

It does not take too long for people to realize that the mysterious “angel echoes” from the sky mainly come from flying birds after World War II [1], [2]. However, plenty of doubts about bird echoes are still haunting. Why are bird echoes blinking [3]? Why does the strength of bird signals fluctuate at a level of about 10 dB [4]? Why are the modulated radar signals of birds correlated with flapping motion [5]? Why does the wingbeat of a bat impart a far more robust amplitude modulation than that of a falcon [6]? Why is there the contradictory that some researchers claim that wings have a negligible effect on bird echoes [7], while some others attempt to extract modulation envelope signatures correlated with the flapping pattern of wings [3], [8] to recognize bird species [9], [10], [11]? All these mysteries about radar echoes from

birds could be attributed to the physics of radar scattering mechanisms from bird targets.

There was once a controversy about the modulation mechanism of birds' signals fluctuation. Shortly after the detection of radar echoes from flying birds by using radar systems [1], people recognize the periodic fluctuation in radar signals of birds in flight [3], [5], [12]. Nevertheless, the modulation mechanism of birds' signal fluctuation is still poorly understood. Many explanations have been proposed successively in the early radar ornithology. The primary empirical evidence believes that there is periodic time series amplitude modulation of radar echoes, and the signal intensities of bird echoes fluctuate as high as 10 ~ 20 dB, even over 40 dB at some radar bands [3], [4], [8]. Since amplitude fluctuation was correlated with the falling of the bird's wings, the flapping pattern of birds is believed to be the primary cause [9], [13]. Nevertheless, periodic variation in scattering areas due to the bird's respiration motion is also a potential explanation [5], [9]. Many researchers have verified that respiration is not

The associate editor coordinating the review of this manuscript and approving it for publication was Chengpeng Hao .

believed to be essential for amplitude modulation [4], [14], and flapping motions causes significant periodic fluctuations in radar signals from flying birds [15], [16], [17], [18]. Yet, some literature still refers to the respiration cause [9], [13].

To date, most scattering models of birds have been based on simple shapes like spheres, cylinders, and spheroids. The most widely scattering model is the water sphere model. Moon developed it to analyze scattering characteristics of birds, in that the radar reflectivity of a bird is predominantly due to the 65% of its mass that is water, and an approximate model of the RCS can be obtained by regarding the bird as a water sphere of equivalent mass to the water content [19]. Some research groups recently proposed complex scattering models with realistic shapes and material properties [17], [20]. However, more theoretical and modeling work is still needed, as well as the labs and field measurements of as many species as possible. Accurate scattering models should be developed to estimate Radar Cross-Section (RCS) values and quantify radar signatures for identifying bird signals and estimating migratory bird density using radar systems.

To subside the controversy about the modulation mechanism of birds' signals fluctuation, we measure the signal fluctuations in radar echoes of flying birds in a microwave anechoic chamber. Current measurements often measure static birds in labs or fields, such as the famous water sphere model birds' test was static without flapping wings [19]. They may neglect the contributions from flapping wings. Unlike them, we estimate the time series of radar echoes from the static & dynamic birds and track dynamic radar signals produced by the flapping gaits of birds. We design a dynamic measurement composed of a network analyzer and a high-speed camera to capture the moment photo of flapping gaits and the corresponding signals for the first time. We also utilize the High-Resolution Range Profile (HRRP) of birds using ultra-wideband signals to separate radar signals of flapping wings from other parts of the bird within multi-bands. Finally, we analyze the data in section III, discuss the results in section IV, and then propose our conclusion that flapping wings contribute to the main signal fluctuations to radar echoes from flying birds, and the contribution can be as high as over 10 dB in section V.

## II. MATERIALS AND METHODS

### A. SCATTERING MODEL

The most impressive scattering theory about birds is that the water in blood and muscles is mainly responsible for the echo produced by a bird, while the reflectivity of feathers seems to be negligible. Radar ornithology usually treats a bird as a water sphere or near-to-spherical target for a simple comparison of target size and wavelength. According to the water sphere model [19], when the mass of a bird is  $m$ , the density of the "bird water" is  $\rho$ , and the radius of the water sphere is given by

$$r = \sqrt[3]{\frac{39m}{80\pi\rho}} \quad (1)$$

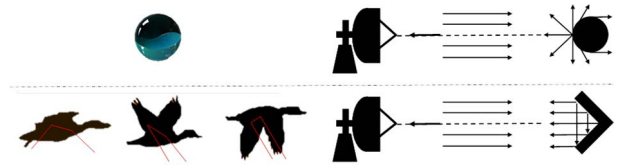


FIGURE 1. Comparison between the traditional water sphere model and our wingbeat corner reflector (WCR) model.

Theoretically, the RCS of a sphere is calculated by [21]

$$\sigma = \pi r^2 \quad (2)$$

Thereby, the theoretical RCS value of a bird based on the water sphere model is calculated by

$$\sigma_b = \pi \left( \frac{39m}{80\pi\rho} \right)^{\frac{2}{3}} \quad (3)$$

Note that the water sphere model completely ignores the contribution from the flapping wings.

Our early project proposes that the time-varying wing-beat corner reflector (WCR) effect could modulate radar echoes from flying birds and contribute a lot to radar received power [22]. Due to the flapping motion, the bird's wing and body constitute a biological corner reflector (Figure 1). This corner reflector effect can significantly amplify the amplitude of the radar echoes from the target; thus, the WCR can enhance backscattering power up to at least 10 dB relative to the cross-section area of a bird [22]. According to the WCR model, the theoretical RCS value of a bird contributed by flapping wings is given by

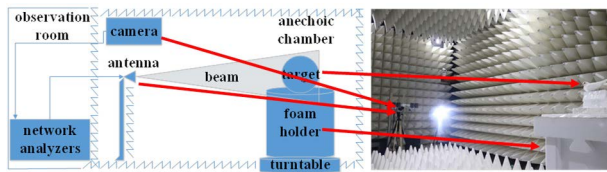
$$\sigma_w = \frac{8\pi a^2 b^2}{\lambda^2} \phi \quad (4)$$

Thereby, considering RCS parts from both the bird body ( $\sigma_b$ ) and the wingbeats ( $\sigma_w$ ), the theoretical RCS value of a bird is given by

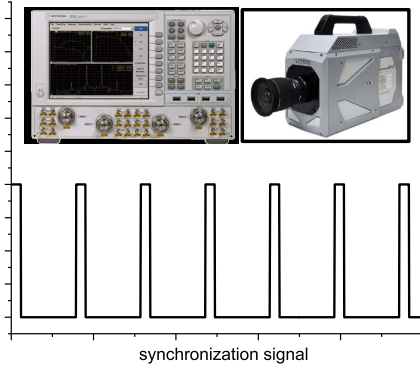
$$\sigma_c = \sigma_b + \sigma_w = \pi \left( \frac{39m}{80\pi\rho} \right)^{\frac{2}{3}} + \frac{8\pi a^2 b^2}{\lambda^2} \phi \quad (5)$$

where,  $\sigma_b$  is the RCS values from the bird body;  $\sigma_w$  is the RCS values from the wings;  $a$  is the length of the corner face;  $b$  is the width of the corner face;  $\lambda$  is the wavelength;  $\phi$  is the function related to the phased angle of flight gaits and observation angle of the radar beam. Compared to equation (3), equation (5) indicates that the RCS value of a flying bird is the sum of both the bird's body and the beats wings.

The contribution from flapping wings to the bird RCS is much more significant than that from the bird body. Take a duck as an example. In 2010, the FAA published the radar advisory circular 150/5220-25 to instruct the design and use of avian radar systems to supplement an airport's Wildlife Hazard Management Plan and reduce the potential bird strike hazards to aircraft [23]. The FAA utilized the Standard Avian Target (SAT) to evaluate the performance of an avian radar system. One SAT bird approximates an average crow with



(a) spatial arrangement in the anechoic chamber and a photo of a bird



(b) the VNA and camera synchronized by the signals

FIGURE 2. Dynamic measurement system.

0.5 kg mass and  $0.025 \text{ m}^2$  RCS [23], and a multiple SAT bird has increased or decreased RCS and mass quantities accordingly. A duck is treated as a two SAT bird with a 1 kg mass. According to the water sphere model [19], [24], the water sphere of the duck is about 0.65 kg, with the density of the water sphere being  $1 \text{ g/cm}^3$ , and the radius is about 5.4 cm; thus the  $\sigma_b$  of the 1kg duck is  $0.0313 \text{ m}^2$ , similar to  $0.05 \text{ m}^2$ , as reported by the FAA [23]. However, according to our WCR model, considering that both  $a$  and  $b$  of the duck are 5.4 cm, and the typical wavelength of the X band is 3 cm; thus, its maximum  $\sigma_w$  is  $0.2375 \text{ m}^2$ . Thus, the contribution from flapping wings ( $\sigma_w$ ) is bigger than that from bird body ( $\sigma_b$ ) by about 659%. In total, the RCS value ( $\sigma_c$ ) of a 1kg duck is  $0.2688 \text{ m}^2$ , approximate 10 times than that ( $\sigma_b$ ) based on the water sphere model.

### B. DYNAMIC MEASUREMENT SYSTEM

Firstly, we extract the weak radar signals of birds in an anechoic chamber. Compared to radar signals of aircraft, radar echoes of birds are weak. We prefer measurement in an anechoic chamber than in the field test. The anechoic chamber belongs to National Center Marine Equipment Quality Inspection, China. The website of this anechoic chamber is <http://www.chinanmei.com/>. FRANKONIA Inc. manufactures the main equipment for this anechoic chamber. The inter size of this room is  $7.890 \times 3.517 \times 3.3\text{m}$ . Furthermore, vector network analyzers (VNA) have become convenient for onsite measurements [25]. The spatial arrangement in the anechoic chamber is shown in Figure 2a. We use the network analyzer of the Agilent N5224A as the radar, as shown in Figure 2b. The network analyzer works in vertical polarization to transmit signals and receive echoes. The biggest advantage of tests in an anechoic chamber is to lower possible background

clutter and improve the scattering power of the signals of cooperative targets.

Secondly, to separate radar signals of wings from the bird body, we utilize the High-Resolution Range (HRRP) technology which transmits the ultra-wideband radar signals. When the bandwidth of swept frequency ( $B$ ) is broad, the range resolution ( $r_{es}$ ) will be narrow enough to achieve the HRRP of a target [21]. The equation is given by,

$$r_{es} = \frac{c}{2B} \quad (6)$$

where  $c$  is the transmission velocity, network analyzers provide the function of swept frequency to obtain the HRRP. Most surveillance radar systems used for detecting birds work with low-resolution range profiles (LRRP). LRRP cannot provide details about the scattering centers of birds and their modulation on radar signatures [26], [27]. Measurements in labs serve the detection of an existing radar system in practice. Since most radars used for monitoring flying birds are either weather surveillance radar systems, marine navigation radar systems, or surface surveillance radar systems [28], [29], we also select some typical surveillance radar bands. Surveillance radar bands are mainly sorted into two categories: those radar wavelengths are similar to general bird sizes, such as S-band and L-band; others are much smaller than available bird sizes, for example, X-band, and Ku-band. Radar data within the former fail into the resonance region, while the latter is into the optic region [2], [30]. Scattering rules differ in the two scattering regions, and not all radar bands are helpful to detect radar echoes from flying birds. To investigate the difference within the scattering regions, we use S- band ( $2 \sim 4\text{GHz}$ ), X-band ( $8 \sim 12\text{GHz}$ ), and Ku-band ( $14 \sim 18\text{GHz}$ ), considering the general size of the birds.

Thirdly, to record the detailed flapping gaits of birds, we deploy a high-speed camera to record the deformation during the whole experiment. The camera is FASTCAM SA-Z (Figure 2b), manufactured by Photron Inc. from Japan. It provides megapixel image resolution at frame rates up to 21,000 frames per second (fps). The flapping rates of small birds are about 6-10 Hz, while that of a large duck is much slower. Since the flapping rate of birds is smaller than the sampling rate of the camera, the camera with a high-speed sampling rate can capture the detailed deformation. Besides, we use tape to fix the legs of birds. We found that the birds were quieter than we thought. When we placed a bird on the foam holder shown in Figure 2, the bird would not move its head or fly away from the foam holder. It just stayed quietly on the foam holder. As such, we can quickly obtain the radar signatures posed by the flapping motions by combining radar echoes with the correspondent photos.

Fourthly, considering different bird sizes, we select several typical birds. Table 1 demonstrates the detailed parameters of birds. Generally, bird mass is a helpful criterion for classifying bird size. Regardless of sexual dimorphism, birds  $< 70 \text{ g}$  are categorized as small. Birds between  $71\text{-}800 \text{ g}$  are categorized as a medium, and birds with masses  $> 801 \text{ g}$

TABLE 1. Parameters of birds in the test.

Contents	dove	duck
Mass (g)	400	955
Wingspan (cm)	66	75
Body length (cm)	33	38
Wings width (cm)	10	14
Leg length (cm)	9	18
Beak length (cm)	2	6

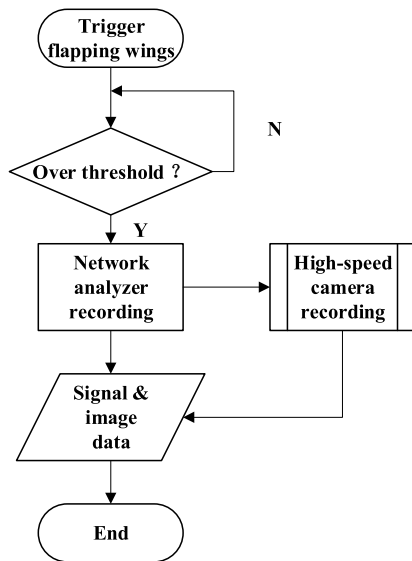


FIGURE 3. Flow-process diagram of one measurement.

are categorized as large [31]. Besides, bird size can be classified using general flight morphology, that large birds habitually carry their feet stretched out behind them during flight, leaving their feet apart from the body and being recognizable to both human observation and radar detection. In contrast, small birds tend to carry their feet drawn up in front, clinging to the body, thus hiding their feet from detection [32]. The dove in this paper is a small bird, and the duck is a large one, either using the taxonomy based on either bird size or the flight morphology. Thereby, the HRRP data of 3.75 cm and 7.5 cm within radar bands can still separate the flapping wings and the body.

Finally, we design an algorithm to automatically record the radar signals of flying birds. Assume the flapping rate is 10 Hz; according to the sampling theorem, the sampling rate of measuring signals should be at least 20 Hz to capture the influence on radar signals of a single flapping gait. Thereby, it requires an algorithm to do the work automatically. The flow-process diagram is shown in Figure 3. It is a threshold detection method. Usually, the VNA continuously transmits radar signals and receives echoes from the birds. At this time, the bird may stay static. And then, we send a signal to stimulate the bird to flap its wings. Since the bird flap its wings, its radar signals change. When the amplitude of the bird’s signal is over the threshold detection of our network analyzer, it begins to send a signal to drive the

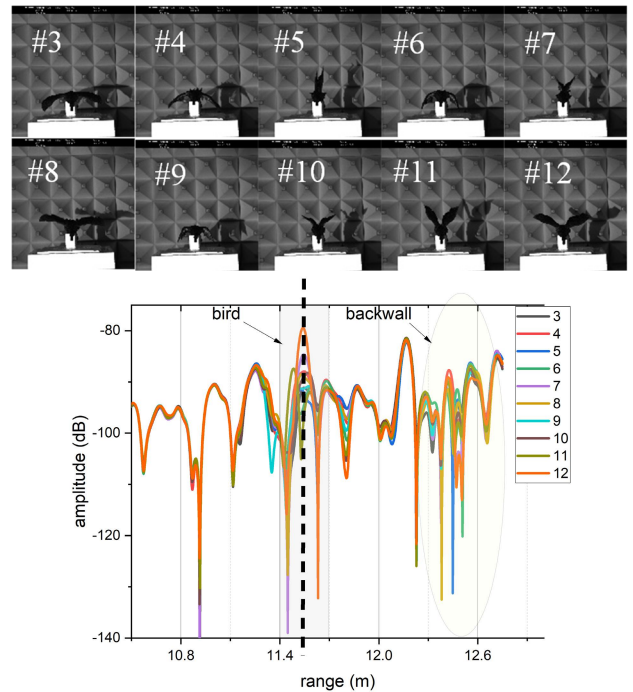


FIGURE 4. Example of the dynamic flapping gaits of birds and their corresponding radar signals within the X-band.

network analyzer and high-speed camera to record the signals and the images. Specifically, we call the Trigger-Aux function of PNA-N5524A to send the synchronistical signals. It can input a trigger signal and then send out two synchronistical response signals (i.e., the synchronization signals in Figure 2b) to external devices using the Handler IO of “Aux Trig out 1” and “Aux Trig out 2” on the panel of PNA-N5524A. The above diagrams of single measurement were functioned using the Macros function of PNA-N5524A. Besides, we deploy a rotating table to measure different angles of birds.

### III. RESULTS

Radar echoes from birds are presented in the range profiles. Figure 4 demonstrates the dynamical measurement of the duck, marked in the light gray frame. We select ten photos of the duck and their corresponding echoes. The numbers on the photos are the tracking number of flight gaits. We remove data #1 and #2 and select ten photos from #3 to #12 because we found that the duck stayed static at the beginning stage of data #1 and #2 in some cases. The test band is an X-band with a range resolution of 3.75 cm. The interval time between the adjacent two frames is 100 ms. In this test, the duck’s chest is in the face of a radar beam, which we call the “front-side” view. As the radar signals are transmitted from port 1 of the VNA, they pass through the cable, the transmit antenna, and the air, and then strike the target. When the backscattering echoes from the target are received by the receiver antenna, they pass the cable and are into port 2 of the VNA. After calculation, the data are presented on the screen of the VNA,



as the example in Figure 4. Thereby, the values of the range axis in Figure 4 describe the radar range between the target and the VNA. These ranges (e.g., 11.4 m) are longer than the inter length of the room (i.e., 7.89 m) because the radar range must count in the cable length. One scan can obtain one HRRP of the target, and the continuous measurements can collect continuous HRRPs, which are corresponding to the changing postures of the target.

There are considerable fluctuations corresponding to the HRRP data of the duck in the light gray frame from 11.4 to 11.8 m in Figure 4. We can find that the duck was only flapping its wings towards the radar wave while its beak moved little, based on the photos of the duck; thereby, the signal fluctuations in the light gray describe the radar signals modulated by the flapping gaits. Furthermore, we use the peaks of the envelope in the gray frame (i.e., the black dotted line in Figure 4) to quantify the contribution of the flapping wings to the scattering power of birds. As shown in Figure 4, the fluctuating range of the signals produced by the flapping wings can be as high as 20 dB, meaning that the flapping wings can contribute 20 dB to the scattering power of flying birds.

The flapping wings contribute a lot to radar echoes from birds regardless of radar bands and radar angle. Figure 5 demonstrates the radar signals of different birds within different radar bands. The recording videos indicate that the duck can flap its wings for about 2-3 seconds in the test, while the dove's flapping time lasts 3-4 seconds. We select the maximum and minimum signals of birds during the flapping time and the mean values of the signals. The minimum signals are the static state of birds, while other data come from the flapping wings.

The difference between the maximum and the minimum can be seen as the contribution of flapping wings. As shown in Figure 5, the contribution of flapping wings can be as high as 20 dB within three radar bands, and the mean contribution is about 10 dB. Besides, due to the flapping wings, the whole bird's HRRP turns to fluctuate. The scope of the fluctuations becomes wide, even wider than the bird size (i.e., 40 cm). Radar bands seem to influence the size of contributions. The magnitudes of radar signals within the S-band are the highest, X-band is the second, and Ku-band is the lowest. However, the contributions within S-band are the smallest, and that within Ku-band is the strongest, up to over 20 dB. The higher the radar frequency comes, the higher contributions produced by the flapping wings.

These results of three radar bands are in accordance with the theoretical ones based on equation (5), which is that the RCS values of the corner reflector are inversely proportional to the square of the wavelength. Besides, since the broad view can only capture contributions of one wing, the fluctuations signals posed by flapping wings are more homogenous than that in the front view. Considering the contributions within the same radar band and same view angle, the contributions of the duck are smaller than that of the dove. Contributions seem to be inversely proportional to the bird size. It is also

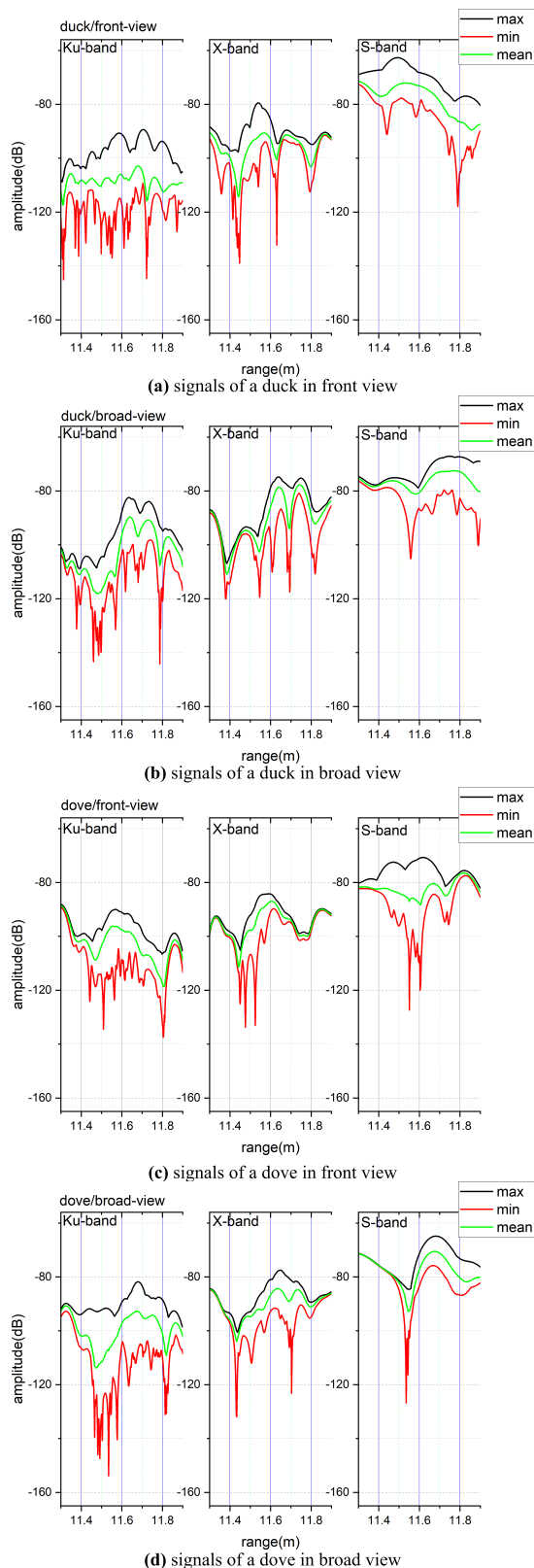
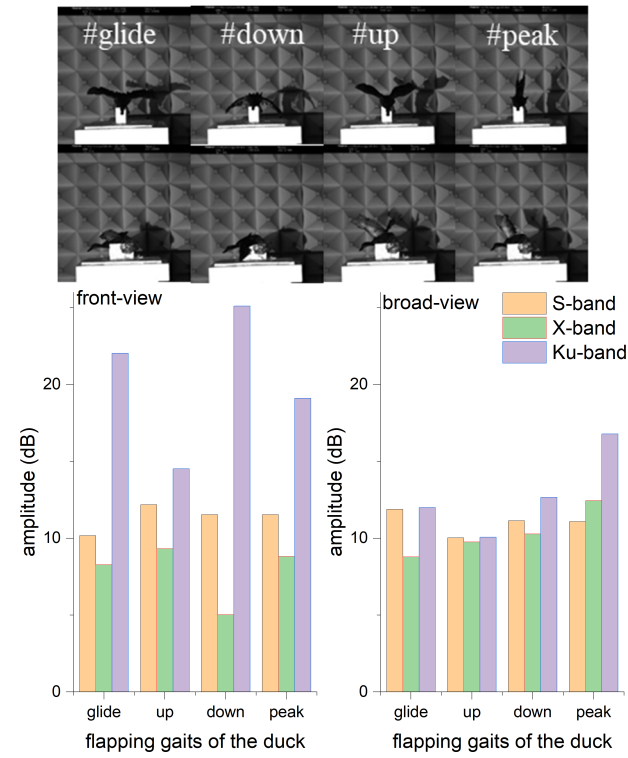
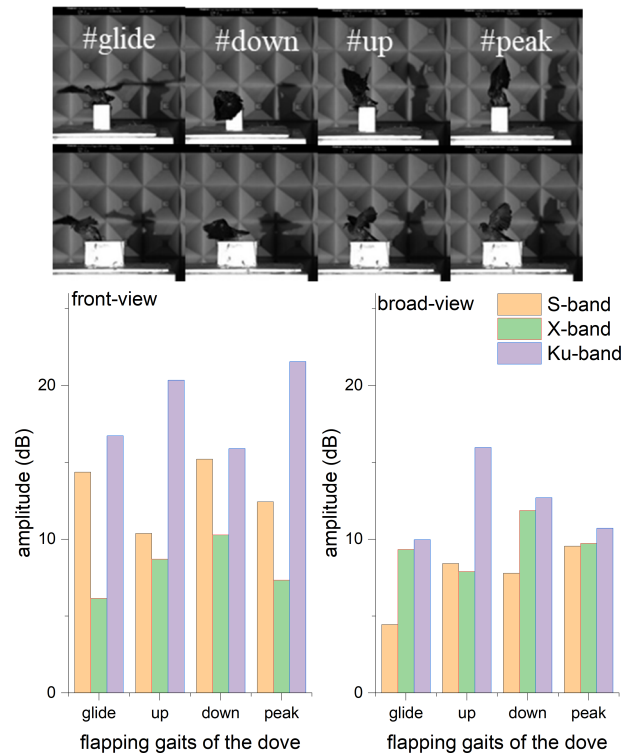


FIGURE 5. Maximum and minimum fluctuating signals modulated by the flapping wings.

reasonable. Small birds have a higher flapping rate than large birds. When the sampling frequency is the same, the higher



(a) contributions to radar signals from the duck's different flapping gaits



(b) contributions to radar signals from the dove's different flapping gaits

**FIGURE 6. Contributions to radar signals from different flapping gaits of birds.**

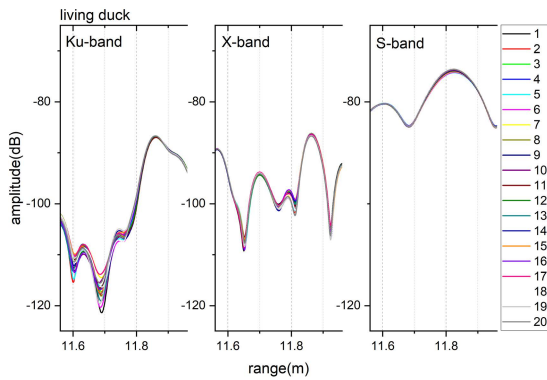
wingbeat frequency will achieve a higher detection rate of the WCR and obtain a higher contribution from flapping wings.

The contributions are related to the flapping gaits of birds. Figure 6 shows the signal fluctuations within three radar bands, which are correlated to different flapping gaits of both the duck and the dove. We select four flapping gaits based on the high-speed photos demonstrated in Figure 6. The four flapping gaits include “glide,” “down,” “up,” and “peak.” The “glide” one is the bird stretching out its wings as gliding flying. The “up” and “down” ones mean the bird flaps its wings upstroke and downstroke, respectively. Moreover, the “peak” gait represents the bird flapping its wings at the peak phase, when the two wings seem to touch each other, as shown in the fourth photo in one line of Figure 6. The signal fluctuations between dynamic flapping and static gait in Figure 6 are different. The values are the mean number calculated with the signals across the range span of 10-cm where the bird was located.

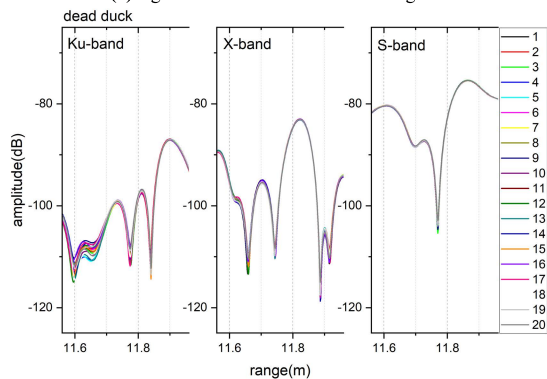
The results indicate that almost all contributions are over 10 dB within three radar bands, regardless of bird species and observation angles. In addition, the mean fluctuations within the Ku-band are still the strongest in the same condition. Besides, the mean contributions in the front view are bigger than that in the broad view regarding bird species. Although there is no linear function between the flapping gaits and the mean fluctuation, the fluctuations of “down” are the most common ones that bring about the strongest fluctuations. Compared to other gaits, the downstroke could cause the corner reflector deformation at the highest rate, making the strongest contributions.

The over 10-dB signal fluctuation comes not from the respiration movement of birds. There was once a claim that respiration may contribute to the 10 dB signal fluctuation in radar echoes from birds. To oppose this claim, we also compare radar data of a living duck with a dead duck. Figure 7 demonstrates the comparison of signal fluctuations of a living duck and a dead duck. They had similar mass and body. We select 30 continuous photos of the birds and their corresponding echoes within three radar bands. The intervals between the sampling frames are about 100 ms, and the whole 30 frames cost about 3 seconds. The chest of the duck faces the radar wave. Besides, the breathing rate of the duck was higher than the average state because the data were sampled after the duck thronging strenuous exercise, and the high-speed photos captured the apparent breathing motion of the chest.

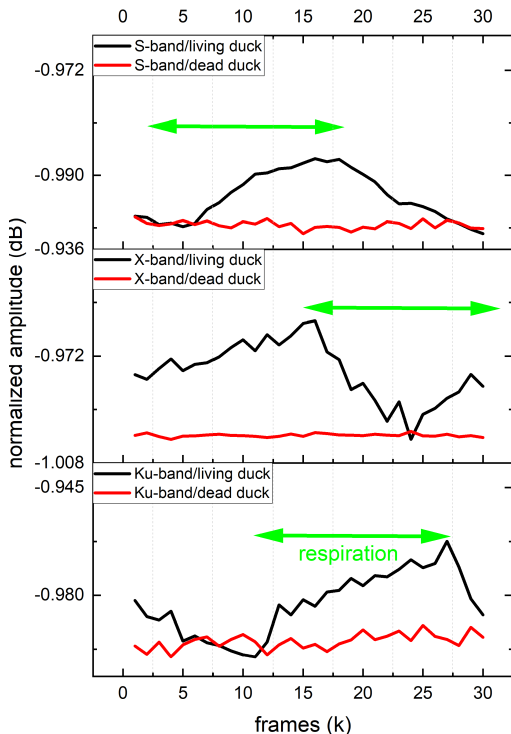
As shown in Figure 7c, the measured respiration period was about 1500 ms, meaning that the respiration rate of the duck is about 0.67 Hz. The respirations do cause some fluctuations in the radar signals from the bird, but the fluctuations are small. The signal fluctuations of the dead duck are no more significant than 1 dB within any measured radar band. However, the respirations of the chest cause different levels of signal fluctuations in radar data within three radar bands. The level is less than 1 dB within S-band, up to 5 dB within X-band, and around 2 dB within Ku-band. In brief, respiration motions are not responsible for the 10 dB level of fluctuation in radar echoes from flying birds.



(a) signal fluctuations of a static living duck



(b) signal fluctuations of a static dead duck



(c) tracking normalized signal fluctuations modulated by the respiration

**FIGURE 7.** Comparison of signal fluctuations of a living duck and a dead duck.

**IV. DISCUSSION**

The 10 dB signal fluctuation within radar signals of flying birds comes from the flapping wings over the respirations.

The radar band is the first factor affecting the contribution produced by the flapping wings. Generally, the higher frequency, the stronger contribution due to flapping wings. It is because of the scattering regions [21], [33]. Only in the optic region, can the WCR work well because of the “scattering centers” theory. Scattering power in S-band may come mainly from a target’s materials component, which is explained using the “scattering polar” theory. Equation (5) also indicates that the theoretical RCS of a corner reflector is inversely proportional to the square of the wavelength. Nevertheless, an exception still exists in contribution within the X-band in Figure 6. Note that the contribution of the X-band is smaller than that of the S-band sometimes. This case could be explained that the scattering within X-band is so complex that the scattering region may come between the resonance region and the optic one. Thus, the contribution of flapping wings is hard to quantify using one scattering theory.

Theoretically, the contribution of flapping wings can be related to each flying gait using this paper’s dynamic measurement system. However, due to the imitated sampling rate of measurement provided by the network analyzer, PNA-N5524A, it cannot achieve the theoretical of 20 Hz, considering the wingbeat frequency of 10 Hz. The quickest measurement rate of PNA-N5524A is only 10 Hz. Therefore, the sub-sampling rate causes the noncontinuous photos and signals produced by the inhomogeneous flapping gaits. Thereby, the results in Figure 4 jump between the adjacent flapping gaits. Nevertheless, the dynamic measurement system still captures and records the moment of birds’ flapping gait and the corresponding radar signals. Thus, we can build the relationship between the radar signals and the flapping gaits and quantify the contributions to birds’ radar signals produced by the flapping wings.

For a single bird, the wingbeat corner reflector effect will amplify bird signal intensity (or RCS) considerably up to 10 dB. RCS is a measure of a target’s efficiency for scattering radiation back to its source; in other words, RCS represents the size of the target as “seen” by the radar [21]. Our measurements show that a 0.35kg flying pigeon can be detected at 12 km [35], and its mean RCS value is 0.25 m<sup>2</sup>, which is considerably more significant than that of 2km and 0.025 m<sup>2</sup> proposed by the FAA [23]. It is 10 dB from 0.025 m<sup>2</sup> (i.e., -16.02 dBsm) to 0.25m<sup>2</sup>(i.e., -6.02 dBsm), which is consistent with the theoretical contribution of a WCR. Moreover, when the bird’s aspect angles are front side to the radar beam compared with head- or tail-on, the wingbeat corner reflector does the strongest effect as a corner reflector; thus, bird RCS is measured higher as provided in this aspect [14], [20].

For different bird species, wingbeat frequency and wing shape affect the modulation effect of the wingbeat corner reflector. As the wingbeat frequency tends to increase with bird size [34], a little bird beats its wingbeat frequency faster than a large one. For example, the large seagull only does 5 wingbeats in one second, while the little starling completes 12 flapping cycles. Under the same conditions, quicker wingbeats increase the stability of the wingbeat corner reflector

effect, and then a little bird (e.g., a pigeon) tends to reap a higher echo strength value than a large bird (e.g., a crane). Besides, the more corner-like wings, the better the wingbeat corner reflector effect is because the perpendicular wings enhance the modulation effect. Therefore, even for a similar bird, a Laridae-like bird embraces a much bigger RCS than a Fringillidae-like bird. This is the same reason that the wingbeat of a bat imparts a far more robust amplitude modulation than that of a falcon [6].

The WCR theory can explain the phantom ripple flicker of “angel echoes” for a flock of birds. Numerous bird species travel in highly organized groups [35] and flap their wings at different gaits to cope with the dynamic wakes produced by flapping wings [36]. When the radar detects the flock, there are always two or more birds in the radar pulse volume, and then it is hard to tell how many and how strong the WCR of each bird in the flock are contributing. Consequently, the whole reflectivity can fluctuate rather violently from 20 dBz levels to 30 dBz levels [37], producing annoying wax and wane along the migrating trajectory on the radar display [1].

## V. CONCLUSION

We design a dynamic measurement system using the network analyzer and the high-speed camera to quantify the signal fluctuations and find the primary cause. There is over 10 dB signal fluctuation in radar echoes from flying birds. Since the respiration motion can cause 5 dB fluctuations at most within different radar bands, the respiration is not the source of the 10 dB fluctuation. Compared to the respiration motion, the flapping wings contribute at least 10 dB to the signal fluctuation to the radar echoes from flying birds, regarding different radar bands, observing angles, and bird species. The contribution is related to the flapping gaits. These results indicate that the time-varying wingbeat corner reflector is proper to explain the modulation mechanism of the 10 dB signal fluctuations in radar ornithology. Moreover, the wingbeat corner reflector effect can answer many mysteries about bird echoes in radar ornithology.

## ACKNOWLEDGMENT

The authors would like to thank the assistants at Marine Equipment Inspection and Testing Company in Qingdao, China, including Wenjing Bao and Shangde Wu.

## REFERENCES

- [1] A. D. Fox and P. D. L. Beasley, “David lack and the birth of radar ornithology,” *Arch. Natural Hist.*, vol. 37, no. 2, pp. 325–332, 2010, doi: [10.3366/anh.2010.0013](https://doi.org/10.3366/anh.2010.0013).
- [2] S. A. Gauthreaux, “Radar ornithology and biological conservation,” *Auk*, vol. 120, no. 2, pp. 266–277, Apr. 2003, doi: [10.2307/4090179](https://doi.org/10.2307/4090179).
- [3] L. L. Bonham and L. V. Blake, “Radar echoes from birds and insects,” *Sci. Monthly*, vol. 82, no. 4, pp. 204–209, Apr. 1956. [Online]. Available: <http://www.jstor.org/stable/21945>
- [4] C. R. Vaughn, “Birds and insects as radar targets: A review,” *Proc. IEEE*, vol. 73, no. 2, pp. 205–227, Feb. 1985, doi: [10.1109/PROC.1985.13134](https://doi.org/10.1109/PROC.1985.13134).
- [5] G. W. Schaefer, “Bird recognition by radar: A study in quantitative radar ornithology,” in *The Problems of Birds as Pests*. London, U.K.: Academic, 1968, pp. 53–86, doi: [10.1016/b978-1-4832-2869-3.50013-9](https://doi.org/10.1016/b978-1-4832-2869-3.50013-9).
- [6] A. Feduccia, “Is it a bird? Is it a dinosaur?” *New Scientist*, vol. 214, no. 2862, pp. 28–29, 2012, doi: [10.1016/s0262-4079\(12\)61084-7](https://doi.org/10.1016/s0262-4079(12)61084-7).
- [7] P. Blacksmith and R. B. Mack, “On measuring the radar cross sections of ducks and chickens,” *Proc. IEEE*, vol. 53, no. 8, p. 1125, Aug. 1965, doi: [10.1109/PROC.1965.4117](https://doi.org/10.1109/PROC.1965.4117).
- [8] T. G. Konrad, J. J. Hicks, and E. B. Dobson, “Radar characteristics of birds in flight,” *Science*, vol. 159, no. 3812, pp. 274–280, Jan. 1968, doi: [10.1126/science.159.3812.274](https://doi.org/10.1126/science.159.3812.274).
- [9] B. Bruderer and A. G. Popa-Lisseanu, “Radar data on wing-beat frequencies and flight speeds of two bat species,” *Acta Chiropterologica*, vol. 7, no. 1, pp. 73–82, Jun. 2007. [Online]. Available: <https://www.ingentaconnect.com/content/miiz/actac/2005/00000007/00000001/art00007>
- [10] B. Bruderer, D. Peter, A. Boldt, and F. Liechti, “Wing-beat characteristics of birds recorded with tracking radar and cine camera,” *IBIS*, vol. 152, no. 2, pp. 272–291, Apr. 2010, doi: [10.1111/j.1474-919X.2010.01014.x](https://doi.org/10.1111/j.1474-919X.2010.01014.x).
- [11] S. Zaugg, G. Saporta, E. Van Loon, H. Schmaljohann, and F. Liechti, “Automatic identification of bird targets with radar via patterns produced by wing flapping,” *J. Roy. Soc. Interface*, vol. 5, no. 26, pp. 1041–1053, Mar. 2008, doi: [10.1098/rsif.2007.1349](https://doi.org/10.1098/rsif.2007.1349).
- [12] S. Rahman and D. A. Robertson, “Radar micro-Doppler signatures of drones and birds at K-band and W-band,” *Sci. Rep.*, vol. 8, no. 1, p. 17396, Dec. 2018, doi: [10.1038/s41598-018-35880-9](https://doi.org/10.1038/s41598-018-35880-9).
- [13] R. P. Larkin, “Flight speeds observed with radar, a correction: Slow ‘birds’ are insects,” *Behav. Ecol. Sociobiol.*, vol. 29, no. 3, pp. 221–224, 1991, doi: [10.1007/BF00166405](https://doi.org/10.1007/BF00166405).
- [14] B. Torvik, A. Knapkog, O. Lie-Svendsen, K. E. Olsen, and H. D. Griffiths, “Amplitude modulation on echoes from large birds,” in *Proc. 11th Eur. Radar Conf.*, Oct. 2014, pp. 177–180, doi: [10.1109/EuRAD.2014.6991236](https://doi.org/10.1109/EuRAD.2014.6991236).
- [15] T. C. Williams and J. M. Williams, “A Peterson’s guide to radar ornithology,” *Amer. Birds*, vol. 34, no. 5, pp. 738–741, 1980.
- [16] B. Bruderer, T. Steuri, and M. Baumgartner, “Short-range high-precision surveillance of nocturnal migration and tracking of single targets,” *Isr. J. Ecol. Evol.*, vol. 41, no. 3, pp. 207–220, Apr. 1995. [Online]. Available: <https://www.tandfonline.com/doi/citedby/10.1080/00212210.1995.10688794?scroll=top&needAccess=true>
- [17] B. Torvik, K. E. Olsen, and H. D. Griffiths, “X-band measurements of radar signatures of large sea birds,” in *Proc. Int. Radar Conf.*, Oct. 2014, pp. 1–6, doi: [10.1109/RADAR.2014.7060266](https://doi.org/10.1109/RADAR.2014.7060266).
- [18] M. Wang, C. Zhang, and X. Zhang, *Feature Analysis and Research on Radar Target Scattering Characteristics of Typical Individual Migratory Bird*, vol. 348. New Delhi, India: Springer 2016, doi: [10.1007/978-81-322-2580-5\\_46](https://doi.org/10.1007/978-81-322-2580-5_46).
- [19] J. R. Moon, “Effects of birds on radar tracking systems,” in *Proc. IEE Conf.*, vol. 490, Oct. 2002, pp. 300–304, doi: [10.1109/RADAR.2002.1174701](https://doi.org/10.1109/RADAR.2002.1174701).
- [20] S. S. Army and J. D. Warren, “Quantitative ornithology with a commercial marine radar: Standard-target calibration, target detection and tracking, and measurement of echoes from individuals and flocks,” *Methods Ecol. Evol.*, vol. 8, no. 7, pp. 860–869, Jul. 2017, doi: [10.1111/2041-210X.12699](https://doi.org/10.1111/2041-210X.12699).
- [21] P. Tait, *Introduction to Radar Target Recognition*. London, U.K.: Institution of Electrical Engineers, 2006, doi: [10.1049/PBRA018E](https://doi.org/10.1049/PBRA018E).
- [22] J. Gong, J. Yan, D. Li, and R. Chen, “Using the wingbeat corner reflector effect to increase detection range of avian radar systems,” *IET Radar, Sonar Navigat.*, vol. 13, no. 10, pp. 1811–1815, Oct. 2019, doi: [10.1049/iet-rsn.2019.0002](https://doi.org/10.1049/iet-rsn.2019.0002).
- [23] U.S. Department of Transportation. (2005). *Airport Avian Radar Systems—Advisory Circular*. [Online]. Available: [https://www.faa.gov/documentLibrary/media/Advisory\\_Circular/150\\_5220\\_25.pdf](https://www.faa.gov/documentLibrary/media/Advisory_Circular/150_5220_25.pdf)
- [24] V. M. Melnikov, R. R. Lee, and N. J. Langlieb, “Resonance effects within S-band in echoes from birds,” *IEEE Geosci. Remote Sens. Lett.*, vol. 9, no. 3, pp. 413–416, May 2012, doi: [10.1109/LGRS.2011.2169933](https://doi.org/10.1109/LGRS.2011.2169933).
- [25] D. Mirkovic, P. M. Stepanian, J. F. Kelly, and P. B. Chilson, “Electromagnetic model reliably predicts radar scattering characteristics of airborne organisms,” *Sci. Rep.*, vol. 6, p. 35637, Oct. 2016, doi: [10.1038/srep35637](https://doi.org/10.1038/srep35637).
- [26] P. Molchanov, R. I. A. Harmanny, J. J. M. de Wit, K. Egiazzarian, and J. Astola, “Classification of small UAVs and birds by micro-Doppler signatures,” *Int. J. Microw. Wireless Technol.*, vol. 6, nos. 3–4, pp. 435–444, Jun. 2014, doi: [10.1017/S1759078714000282](https://doi.org/10.1017/S1759078714000282).
- [27] B. Torvik, K. E. Olsen, and H. Griffiths, “Classification of birds and UAVs based on radar polarimetry,” *IEEE Geosci. Remote Sens. Lett.*, vol. 13, no. 9, pp. 1305–1309, Sep. 2016.



[28] O. Hüppop, M. Ciach, R. Diehl, D. R. Reynolds, P. M. Stepanian, and M. H. M. Menz, "Perspectives and challenges for the use of radar in biological conservation," *Ecography*, vol. 42, no. 5, pp. 912–930, May 2019, doi: 10.1111/ecog.04063.

[29] H. Schmaljohann, "Radar aeroecology—A missing piece of the puzzle for studying the migration ecology of animals," *Ecography*, vol. 43, no. 2, pp. 236–238, 2020.

[30] B. Bruderer, "The study of bird migration by radar Part 2: Major achievements," *Naturwissenschaften*, vol. 84, no. 2, pp. 45–54, 1997, doi: 10.1007/s001140050348.

[31] E. J. Zakrajsek and J. A. Bissonette. (2001). *Nocturnal Bird-Avoidance Modeling with Mobile-Marine Radar*. [Online]. Available: [https://digitalcommons.usu.edu/wild\\_facpub/1188/](https://digitalcommons.usu.edu/wild_facpub/1188/)

[32] J. Gong, J. Yan, D. Li, and R. Chen, "Comparison of radar signatures based on flight morphology for large birds and small birds," *IET Radar, Sonar Navigat.*, vol. 14, no. 9, pp. 1365–1369, Sep. 2020, doi: 10.1049/iet-rsn.2020.0064.

[33] J. Gong, J. Yan, and D. Li, "Comparison of micro-Doppler signatures registered using RBM of helicopters and WSM of vehicles," *IET Radar, Sonar Navigat.*, vol. 13, no. 11, pp. 1951–1955, 2019, doi: 10.1049/iet-rsn.2019.0210.

[34] W. L. Flock and J. L. Green, "The detection and identification of birds in flight, using coherent and noncoherent radars," *Proc. IEEE*, vol. 62, no. 6, pp. 745–753, Jun. 1974, doi: 10.1109/PROC.1974.9513.

[35] R. M. May, "Flight formations in geese and other birds," *Nature*, vol. 282, no. 5741, pp. 778–780, Dec. 1979, doi: 10.1038/282778a0.

[36] S. J. Portugal, T. Y. Hubel, J. Fritz, S. Heese, and D. Trobe, "Upwash exploitation and downwash avoidance by flap phasing in ibis formation flight," *Nature*, vol. 505, no. 7483, pp. 399–402, Jan. 2014, doi: 10.1038/nature12939.

[37] S. A. Gauthreaux and C. G. Belser, "Displays of bird movements on the WSR-88D: Patterns and quantification," *Weather Forecasting*, vol. 13, no. 2, pp. 453–464, 1998, doi: 10.1175/1520-0434(1998)013<0453:DOBMOT>2.0.CO;2.



**DEREN LI** (Senior Member, IEEE) received the M.Sc. degree in photogrammetry and remote sensing from the Wuhan Technical University of Surveying and Mapping, Wuhan University, Wuhan, China, in 1981, and the D.Eng. degree in photogrammetry and remote sensing from Stuttgart University, Stuttgart, Germany, in 1985. He was elected as an Academician with the Chinese Academy of Sciences, Beijing, China, in 1991; the Chinese Academy of Engineering, Beijing; and the Euro-Asia Academy of Sciences, Beijing, in 1995. He is currently with the State Key Laboratory of Information Engineering in Surveying, Mapping and Remote Sensing, Wuhan University. He is also an Academician with the Chinese Academy of Sciences and the Chinese Academy of Engineering. His scientific interests are in the theory and methodology of geo-spatial science. His current research interests include integration of communication, GNSS, and remote sensing.



**JUN YAN** received the Ph.D. degree in photogrammetry and remote sensing from Wuhan University, Wuhan, China, in 2003. He is currently a Professor with the State Key Laboratory of Information Engineering in Surveying, Mapping and Remote Sensing, Wuhan University. His scientific interests include theory and utilization of radar automatic target recognition for bird strike hazards management and other applications.



**HUIPING HU** received the M.Sc. degree in geomatics engineering from the School of Remote Sensing and Information Engineering, Wuhan University. She is currently working with the Wuhan Geomatics Institute, Wuhan. Her research interests include remote sensing, data mining, and GIS.



**JIANGKUN GONG** (Member, IEEE) received the Ph.D. degree in communication and information system from the State Key Laboratory of Information Engineering in Surveying, Mapping and Remote Sensing, Wuhan University, in 2019. His research interests include bird strike hazards management and drone detection using automatic target recognition technology.



**DEYONG KONG** is currently with the School of Information and Communication Engineering, Hubei University of Economics. His research interests include computer simulation, automatic control method, and software engineering.

...